Biochemical and Biophysical Research Communications 431 (2013) 284–290

Contents lists available at SciVerse ScienceDirect

Biochemical and Biophysical Research Communications

journal homepage: www.elsevier.com/locate/ybbrc

eNOS phosphorylation on serine 1176 affects insulin sensitivity and adiposity

Satoshi Kashiwagi [a,1], Dmitriy N. Atochin [a,1], Qian Li [a], Michael Schleicher [b], Terrence Pong [a], William C. Sessa [b], Paul L. Huang [a,*]

[a] Cardiovascular Research Center, Cardiology Division, Massachusetts General Hospital and Harvard Medical School, Boston, MA 02114, USA
[b] Department of Pharmacology and Vascular Biology and Therapeutics Program, Amistad Building, Yale University School of Medicine, New Haven, CT 06536, USA

ARTICLE INFO

Article history:
Received 9 December 2012
Available online 3 January 2013

Keywords:
Nitric oxide
Endothelium
Insulin resistance
Diabetes
Metabolism
Obesity

ABSTRACT

Phosphorylation of endothelial nitric oxide synthase (eNOS) is an important regulator of its enzymatic activity. We generated knockin mice expressing phosphomimetic (SD) and unphosphorylatable (SA) eNOS mutations at S1176 to study the role of eNOS phosphorylation. The single amino acid SA mutation is associated with hypertension and decreased vascular reactivity, while the SD mutation results in increased basal and stimulated endothelial NO production. In addition to these vascular effects, modulation of the S1176 phosphorylation site resulted in unanticipated effects on metabolism. The eNOS SA mutation results in insulin resistance, hyperinsulinemia, adiposity, and increased weight gain on high fat. In contrast, the eNOS SD mutation is associated with decreased insulin levels and resistance to high fat-induced weight gain. These results demonstrate the importance of eNOS in regulation of insulin sensitivity, energy metabolism, and bodyweight regulation, and suggest eNOS phosphorylation as a novel target for the treatment of obesity and insulin resistance.

1. Introduction

Diabetes and obesity are associated with increased risk for atherosclerotic cardiovascular disease [1] due to multiple pathophysiologic links between insulin resistance, obesity, hypertension, and atherogenic dyslipidemia [2,3]. One common feature of these conditions is endothelial dysfunction, caused by a relative deficiency of nitric oxide (NO), which normally serves protective roles in the vasculature [4–6]. Reduced NO bioavailability leads to vasoconstriction, proliferation of vascular smooth muscle cells, recruitment of inflammatory cells, and increased platelet aggregation, all of which contribute mechanistically to atherosclerosis [7]. The importance of normal NO generation has been demonstrated by the phenotypes of mice lacking the endothelial nitric oxide synthase (eNOS) gene [8], which represent an extreme example of endothelial dysfunction, because they lack any endothelial NO production [9–13].

eNOS enzymatic activity is regulated at multiple levels [7,14], including gene transcription and mRNA stability [15], substrate and cofactor availability [16–18], protein–protein interactions with hsp90 and caveolins [19], and post-translational modifications including phosphorylation [20,21]. Among these possible mechanisms, phosphorylation of eNOS protein at S1177 (human amino acid sequence numbering) plays important roles in regulation of its enzymatic activity [20,21]. The corresponding amino acid residue is S1176 in mice; thus, S1176 was modulated in the current report. Insulin, leptin, vascular endothelial growth factor (VEGF), estrogens, statins, and shear stress increase eNOS S1176 phosphorylation by Akt kinase [22–27]. Adipokines that regulate insulin sensitivity and systemic metabolism such as adiponectin and resistin modulate S1176 phosphorylation by AMP kinase [28,29]. The convergence of these diverse metabolic signals and pathways to regulate eNOS activity suggests the importance of eNOS phosphorylation.

In order to study the role of eNOS S1176 phosphorylation *in vivo*, we generated knockin mice that carry a phosphomimetic and unphosphorylatable mutation in the native eNOS gene. Mice carrying these single amino acid substitutions at the S1176 phosphorylation site showed expected effects on blood pressure, NO production, and vascular reactivity. In addition, they also revealed alterations in glycemic response and bodyweight regulation. These novel results indicate that modulation of eNOS phosphorylation significantly influences metabolism and may therefore be a novel target not only for cardiovascular disease, but also diabetes and obesity.

* Corresponding author. Address: Harvard Medical School, Cardiovascular Research Center, Cardiology Division, Massachusetts General Hospital, 149 Thirteenth Street, Charlestown, MA 02129, USA. Fax: +1 617 726 5806.
E-mail address: phuang1@partners.org (P.L. Huang).
[1] These authors contributed equally to this paper.

0006-291X/$ - see front matter © 2013 Elsevier Inc. All rights reserved.
http://dx.doi.org/10.1016/j.bbrc.2012.12.110

2. Materials and methods

2.1. Generation and genotyping of SD and SA knockin mice

We used homologous recombination to generate knockin mice carrying mutations in the eNOS gene. Targeting constructs were engineered to carry specific amino acid substitutions at the S1176 codon in the exon 26 of the eNOS gene to encode alanine (A) or aspartate (D). The constructs also included a neomycin resistance gene flanked by loxP sites for later excision, and a thymidine kinase gene to select against random integration. The region surrounding exon 26 of the eNOS gene was replaced by homologous recombination with the mutated exon and the neomycin resistance gene in mouse J1 ES cells. After germ line transmission, the mice were mated with EIIa-Cre transgenic mice to excise the neomycin gene. Mice were backcrossed to C57BL6 genetic background by a marker-assisted congenic strategy.

We fed male C57BL/6 and eNOS knockin mice ad libitum with a standard chow diet or a high-fat diet (Harlan Teklad, TD88137; 0.2% cholesterol and 42% milk fat) from 5 weeks of age for 8 weeks. All experiments were approved by the Massachusetts General Hospital Institutional Animal Care and Use Committee.

2.2. NO measurement in murine lung endothelial cells

Murine lung endothelial cells (MLECs) were isolated from 8-week-old WT and eNOS knockin mice, and incubated for 30 min with or without 1 μM A23187. Nitrite accumulation was measured by using a chemiluminescence Sievers NO analyzer.

2.3. Measurement of cGMP production in aortic rings

Mouse aortas were pretreated with 200 μM of IBMX, and cGMP extracted and measured using the Amersham cGMP ELISA kit.

2.4. Blood pressure determination

Systemic blood pressure was measured in the common carotid artery using a catheter from pulled PE-10 tubing under isoflurane anesthesia [30].

2.5. Vascular reactivity studies

Carotid arteries were mounted onto glass cannulas in a pressure myograph (DMT), and perfused in physiologic saline (PSS). The vessel diameter was continuously recorded using a video system (IonWizard version 4.4; IonOptix Corp.). After pre-constriction with 10^{-5} M phenylephrine, increasing concentrations of Ach from 10^{-9} to 10^{-5} M were added stepwise to the organ bath. Basal NO production was inhibited by L-N-arginine methyl ester (L-NAME) at 3×10^{-4} M for 30 min. Dose–response curves for SNP from 10^{-9} to 10^{-5} M were measured. Passive diameters were determined by applying Ca^{2+}-free PSS. ACh and SNP relaxation responses were expressed as percentage change in diameter after phenylephrine preconstriction compared with the difference between calcium-free diameter and diameter after phenylephrine constriction.

2.6. Insulin and glucose tolerance tests

At 15 and 16 weeks of age, animals were subjected insulin and glucose tolerance tests, respectively. After 16 h fast, intraperitoneal insulin (1 U/kg of Humulin-R) or glucose (2 g/kg) was administered and blood samples measured for glucose at 0, 15, 30, 60, 120 min using a BREEZE® 2 Blood Glucose Meter (Bayer).

2.7. Biochemical characterization

Serum measurements for insulin, leptin, adiponectin, and MCP-1 were measured by ELISA. Serum lipid analysis was performed by Skylight Biotech Inc. (Akita, Japan) using HPLC.

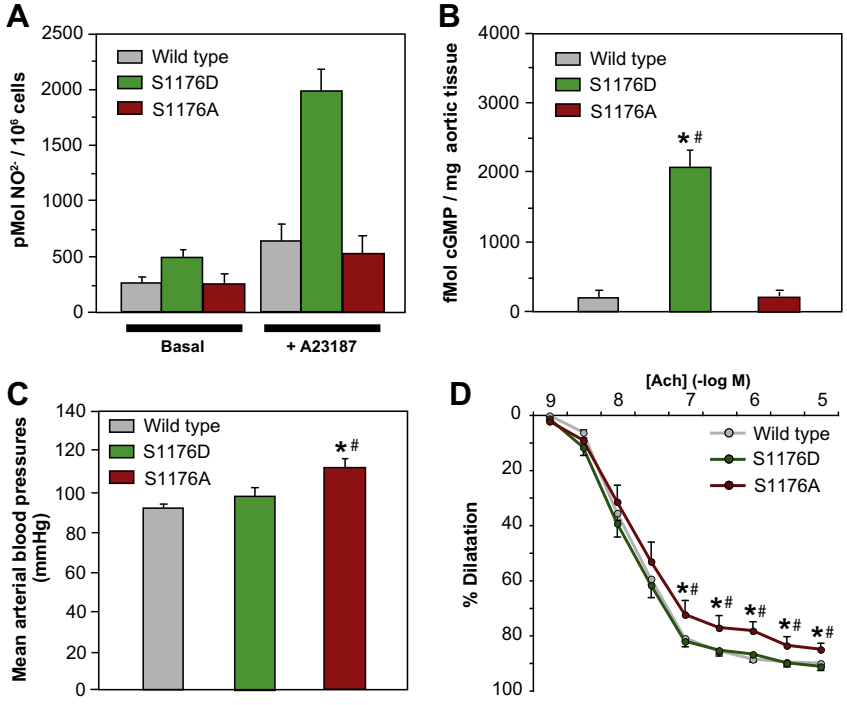

Fig. 1. Effect of phosphomimetic and unphosphorylatable eNOS mutations on NO production, blood pressure, and vascular reactivity. (A) eNOS activity in MLEC at baseline and following stimulation with 1 μM A23187 for 30 min. $n = 4$ for each group. (B) cGMP production in aortic tissue. $n = 3$ for each group. (C) Mean arterial blood pressure of WT ($n = 13$), SD ($n = 10$), and SA ($n = 4$) mice. (D) Vascular reactivity in common carotid arteries of WT ($n = 11$), SD ($n = 8$) and SA ($n = 9$). (A–F) $^{*}P < 0.05$ as compared to WT mice. (A–D) $^{\#}P < 0.05$ versus SA mice. (E–F) $^{\#}P < 0.05$ versus SD mice.

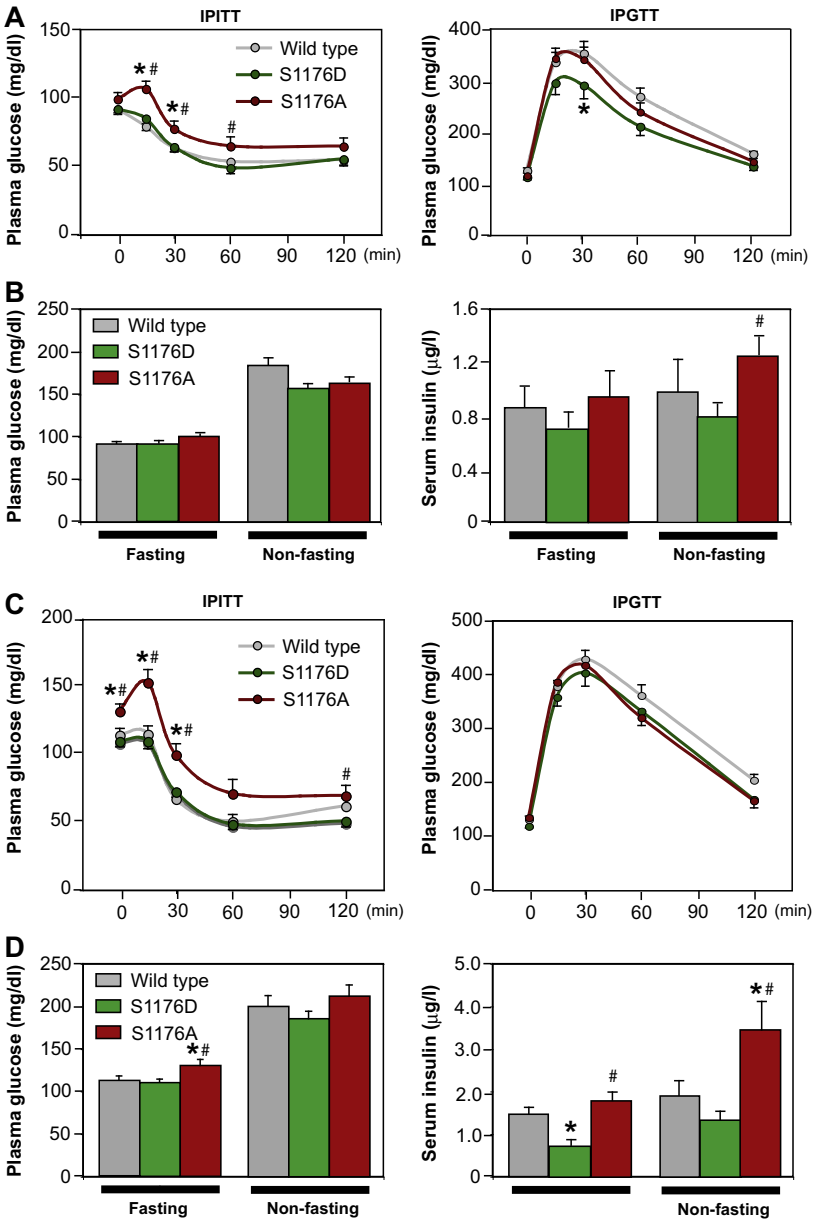

Fig. 2. Effect of phosphomimetic and unphosphorylatable eNOS mutations on insulin sensitivity on regular chow and on high fat diet. (A) Intraperitoneal ITT and GTT of WT and eNOS knockin mice fed a regular chow diet. Left, ITT at 15 weeks in WT (n = 17), SD (n = 36) and SA (n = 25) mice. Right, GTT at 16 weeks in WT (n = 23), SD (n = 33) and SA (n = 28) mice. (B) Fasting and non-fasting plasma glucose levels (left) and serum insulin levels (right) in WT and eNOS knockin mice. (C) Intraperitoneal ITT and GTT of WT and eNOS knockin mice fed a high fat diet. (D) Fasting and non-fasting plasma glucose levels (left) and serum insulin levels (right) in WT and eNOS knockin mice after 8 weeks on high-fat diet. $^{*}P < 0.05$ as compared to WT mice. $^{\#}P < 0.05$ versus SD mice.

2.8. Histology

Paraffin sections (5 μm) of epididymal fat pads were stained with hematoxylin-eosin. Cross-sectional areas of adipocytes were measured using MatLab 7.5 software.

2.9. qPCR analysis

Quantitative real-time PCR was performed using an ABI Prism 7000 (Applied Biosystems) with SYBR Green Master Mix (SABiosciences) and normalized to α-actin.

2.10. Statistics

Data were analyzed by unpaired Student's t-test or one-way analysis of variance (ANOVA) and Bonferroni's post-test as appropriate. Values are expressed as mean ± s.e.m. Statistical significance was set at $P < 0.05$.

3. Results

3.1. Modulation of the eNOS S1176 phosphorylation site affects NO production, blood pressure, and vascular reactivity

We generated knockin mice carrying specific single amino acid substitutions in the native eNOS gene. We mutated the S1176 codon to encode alanine (A) or aspartate (D), resulting in an unphosphorylatable (SA) and a phosphomimetic (SD) mutation. These mutant forms of eNOS have been characterized *in vitro* [20,21], but not *in vivo* in intact animals. Both the eNOS SA and SD mutant knockin mice are viable and fertile. All experiments were performed on animals on C57BL/6 genetic background.

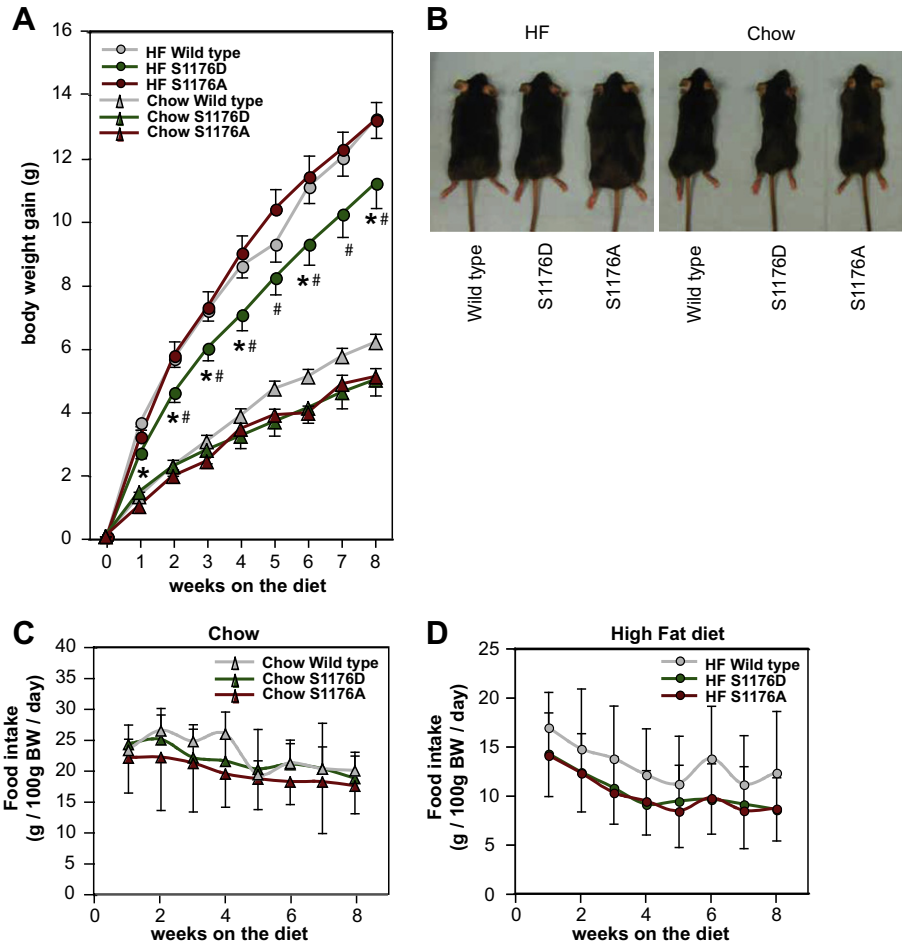

Fig. 3. Effect of phosphomimetic and unphosphorylatable eNOS mutations on weight gain. (A) Weekly weight profile of WT and eNOS knockin mice on regular chow and high fat diet. $n = 22$, 13, and 17 for WT, SD and SA on chow diet, $n = 25$, 22 and 18 on high fat diet, respectively. $^{*}P < 0.05$ as compared to WT mice. $^{\#}P < 0.05$ versus SD mice. (B) Typical appearance of WT and eNOS knockin mice after 8 weeks on high-fat diet (left) and regular chow diet (right). (C) Total weekly food intake of WT ($n = 8$), SD ($n = 9$) and SA ($n = 8$) mice on chow diet. (D) Total weekly food intake of WT ($n = 9$), SD ($n = 11$) and SA ($n = 11$) mice on high fat diet.

Endothelial cells isolated from SD mice showed greater production of NO under basal conditions and after stimulation with the calcium ionophore A23187 than WT or SA mice (Fig. 1A). Cumulative cGMP production in the presence of the phosphodiesterase inhibitor isobutylmethylxanthine (IBMX) was also greater in aortic rings from SD mice than WT or SA mice (Fig. 1B).

Mean arterial blood pressure of eNOS SA mice was higher (111.6 ± 3.7 mmHg) than that of WT (91.8 ± 2.4 mmHg) and eNOS SD mice (98.0 ± 4.4 mmHg), as shown in Fig. 1C. To assess endothelium dependent relaxation, we measured vascular reactivity of isolated pressurized carotid arteries using a myograph in response to acetylcholine (ACh). The vascular reactivity dose–response curve was significantly shifted to the right in SA mice compared with WT or SD mice, indicating reduced vascular relaxation (Fig. 1D).

3.2. S1176 mutations affect insulin sensitivity and glucose metabolism

To determine the effects of eNOS S1176 phosphorylation site on insulin sensitivity and glucose metabolism, we performed intraperitoneal insulin (IPITT) and glucose (IPGTT) tolerance tests on the eNOS knockin mice. On normal chow diet, the ability of insulin to reduce glucose levels was impaired in SA mice compared to SD and WT mice (Fig. 2A, left). In the IPGTT, the SD mice had improved glucose tolerance compared with SA mice and WT mice (Fig. 2A, right). Fasting and non-fasting glucose levels, and fasting insulin levels, were not significantly different among these genotypes (Fig. 2B). The non-fasting insulin level was significantly higher in SA (1.25 ± 0.12 μg/l) mice compared to SD mice (0.79 ± 0.10 μg/l) (Fig. 2B, right). These results suggest that SA mice are able to maintain normal glucose levels and normal IPGTT response despite impaired insulin responsiveness, because of their higher insulin levels. This is similar to the pathophysiology of developing type 2 diabetes in humans. In contrast, the SD mice require less insulin to dispose of plasma glucose upon feeding, indicating higher peripheral insulin sensitivity. Taken together, these results show that modulation of the eNOS S1176 site affects systemic insulin sensitivity and responses to glucose challenge.

In the setting of a high fat for 8 weeks, SA mice displayed a significantly blunted response to insulin, and 15 and 30 min timepoints measured in the IPITT curve were significantly higher than in WT mice and SD mice (Fig. 2C, left). In contrast, there was no significant difference between the IPGTT curves for WT, SA and SD mice (Fig. 2C, right). Fasting and non-fasting glucose levels among all the genotypes were significantly higher than those upon feeding with a chow diet (Fig. 2D, left). After high fat diet, the fasting glucose level of SA (129.7 ± 5.5 mg/dl) was higher than that of SD (110.5 ± 5.0 mg/dl) mice (Fig. 2D, left), while it had been normal with the chow diet. Fasting and non-fasting serum insulin levels of SA mice (1.77 ± 0.26 μg/l and 3.44 ± 0.66 μg/l) were also higher than those of SD mice (0.73 ± 0.19 μg/l and 1.35 ± 0.20 μg/l) and WT mice (1.52 ± 0.22 μg/l and 1.93 ± 0.32 μg/l) (Fig. 2D, right). Thus, high fat diet exaggerates the metabolic abnormalities seen

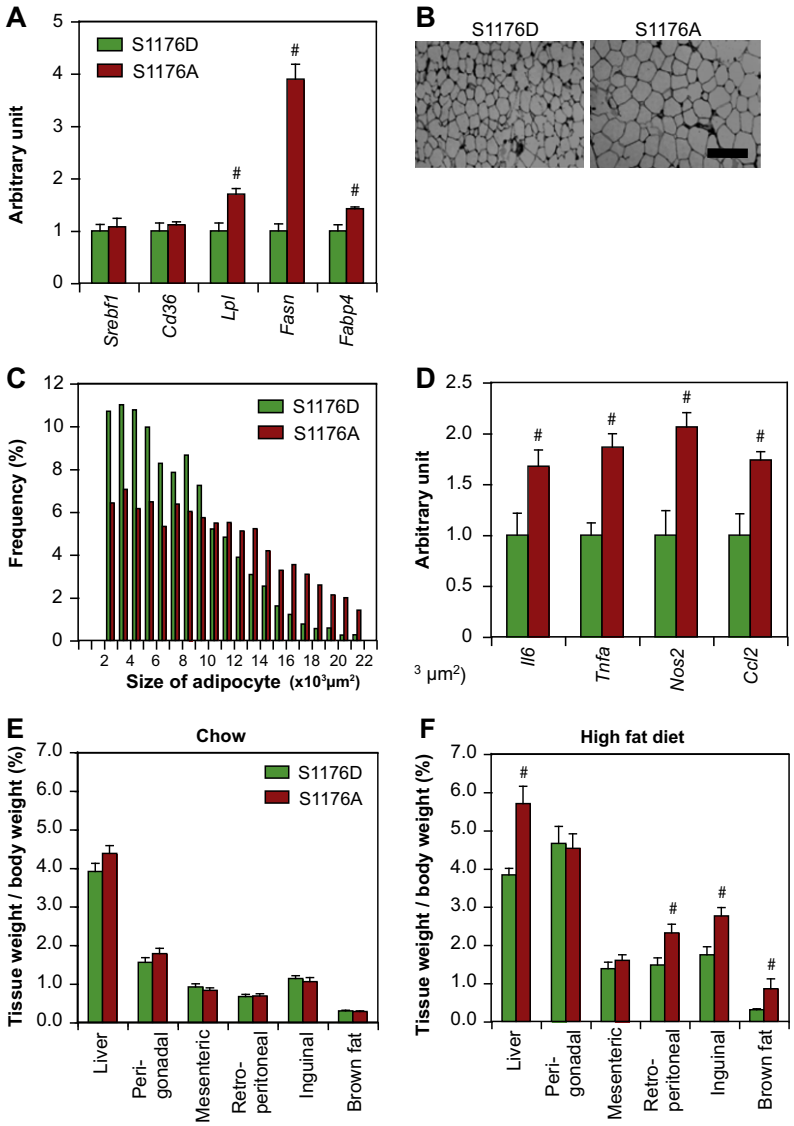

Fig. 4. Energy storage and inflammation in adipose tissue. (A) Expression of markers of fat storage and mitochondrial biogenesis in adipose tissue in SD ($n = 6$) and SA ($n = 6$) mice quantified by qPCR. (B) Histological section of epididymal fat pad. Scale bar 100 μm. (C) Quantification of cross-sectional area of adipose cells in epididymal fat pad. (D) Expression of markers of inflammation in adipose tissue in SD and SA ($n = 6$ each group) mice. (E) Mass of fat depots and liver from SD ($n = 10$) and SA ($n = 9$) mice fed a normal chow diet. (F) Fat depots and liver after 9 weeks of high fat diet. $^{\#}P < 0.05$ as compared with SD mice.

in SA mice, with the development of fasting hyperglycemia and more marked hyperinsulinemia.

Interestingly, the fasting insulin level of SD mice after high fat diet was lower than seen in either WT or SA mice. Insulin levels also remained the same after high fat diet as with a chow diet (0.71 ± 0.13 μg/l versus 0.73 ± 0.19 μg/l) (Fig. 2B and D). These results suggest that SD mice maintain lower insulin levels despite high fat diet. In contrast, the SA mice show diet-induced hyperinsulinemia and decreased insulin sensitivity. Thus, the phosphomimetic SD mutation confers protection against diet-induced insulin resistance, while the unphosphorylated SA mutation is associated with insulin resistance exaggerated by high fat diet.

3.3. eNOS SA mutation is associated with increased weight gain with high fat diet

On a regular chow diet, the growth curves and rates of weight gain were similar among the three genotypes. However, on a high fat diet, SA mice showed a faster increase in weight than SD or WT mice (Fig. 3A and B). The body weight of SA mice was significantly higher than those of WT and SD mice. Total food intake did not differ between the genotypes (Fig. 3C and D).

3.4. Increased energy storage and inflammation in adipose tissue of SA knockin mice

We examined the expression of genes responsible for energy storage in adipose tissue. While expression of SREB F1 and CD36 were the same, LpL, FASN and FABP4, which lie downstream of insulin, were up-regulated in SA mice (Fig. 4A). Histologically, the size of each adipocyte was significantly larger in SA mice compared to that of SD mice ($10.3 \pm 0.4 \times 10^3$ μm^2 versus $6.7 \pm 0.1 \times 10^3$ μm^2) (Fig. 4B and C).

Expression of inflammatory cytokines, such as IL-6, TNF-α, inducible nitric oxide synthase (iNOS), and MCP-1 in adipose tissue was increased in SA mice compared to SD mice (Fig. 4D). Serum MCP-1 concentration was significantly increased in SA mice (Table 1). Adiponectin, which plays a key role in glucose and lipid homeostasis and is decreased in diabetes and metabolic syndrome

Table 1
Effect of eNOS mutation on serum adipokines and lipid profile.

	Chow		HFD	
	S1177D	S1177A	S1177D	S1177A
Fasting leptin (ng/ml)	9.02 ± 3.68 (n = 6)	6.33 ± 3.15 (n = 4)	18.74 ± 4.55 (n = 6)	37.71 ± 5.22[#] (n = 6)
Fasting adiponectin (μg/ml)	8.99 ± 0.43 (n = 6)	6.78 ± 0.83[*] (n = 5)	9.78 ± 0.72 (n = 5)	7.83 ± 0.33[#] (n = 4)
MCP-1 (pg/ml)	14.84 ± 2.02 (n = 11)	45.88 ± 10.48[*] (n = 7)	14.49 ± 2.02 (n = 5)	27.11 ± 6.49[#] (n = 6)
NEFA (mEq/l)	0.32 ± 0.03 (n = 7)	0.43 ± 0.04[*] (n = 6)	0.36 ± 0.04 (n = 3)	0.65 ± 0.19 (n = 4)
HDL (mg/dl)	81.92 ± 7.73 (n = 7)	63.59 ± 5.87 (n = 6)	137.88 ± 14.96 (n = 3)	172.11 ± 7.03 (n = 4)
VLDL (mg/dl)	3.56 ± 0.65 (n = 7)	3.59 ± 0.50 (n = 6)	8.75 ± 1.09 (n = 3)	10.95 ± 1.65 (n = 4)
sLDL (mg/dl)	1.88 ± 0.11 (n = 7)	2.31 ± 0.17 (n = 6)	4.55 ± 0.29 (n = 3)	6.34 ± 0.46[#] (n = 4)
LDL (mg/dl)	9.60 ± 0.60 (n = 7)	11.71 ± 0.82 (n = 6)	25.16 ± 3.99 (n = 3)	42.70 ± 5.52[#] (n = 4)
Tryglyceride (mg/dl)	40.49 ± 10.01 (n = 7)	37.71 ± 4.16 (n = 6)	27.29 ± 9.77 (n = 3)	24.13 ± 5.04 (n = 4)

Values are the mean ± s.e.m.
HFD: high fat diet, MCP-1: monocyte chemotactic protein-1, NEFA: non-esterified fatty acid, HDL: high-density lipoprotein, VLDL: very low-density lipoprotein, sLDL: small low-density lipoprotein, LDL: low-density lipoprotein.
[*] $P < 0.05$ as compared to SD mice on chow diet.
[#] $P < 0.05$ as compared to SD mice on HFD.

[31], was significantly lower in SA mice compared to SD mice (Table 1).

After high fat diet, the masses of fat depots of SA mice were higher than those of SD mice, indicating higher adiposity along with weight gain (Fig. 4E). Serum leptin level of SA mice was also increased (Table 1) as was liver weight. SA mice had elevated low-density lipoprotein (LDL) cholesterol and particularly small dense LDL particles, compared to SD mice (Table 1).

4. Discussion

We report here that single amino acid modifications at the eNOS S1176 phosphorylation site directly affect systemic insulin sensitivity and bodyweight regulation. The unphosphorylatable SA eNOS mutation results in insulin resistance, hyperinsulinemia, and fasting hyperglycemia. SA mice show increased adiposity, expression of inflammatory markers, and increased weight gain on high fat diet. In contrast, the phosphomimetic SD mutation results in decreased insulin levels and protection from diet-induced insulin resistance.

The eNOS SA and SD mice express normal levels of eNOS protein. By mimicking the biological actions of phosphorylated and unphosphorylated states, they can reveal how modulation of the S1176 phosphorylation site affects vascular function. The vascular phenotypes of the mice are consistent with known roles of NO. Endothelial cells from SD mice show greater NO production, greater aortic cGMP content, and lower blood pressure.

S1176 mice show unanticipated phenotypes related to metabolism. SA mice show insulin resistance. When fed a normal diet, they maintain euglycemia in the face of insulin resistance by hyperinsulinemia. When faced with the increased stress of a high fat diet, they are unable to compensate fully for insulin resistance by hyperinsulinemia, resulting in hyperglycemia. In contrast, the SD mice show resistance to the effects of high fat diet and maintain insulin sensitivity and a lean phenotype.

NO is an important downstream effector of insulin signaling. NO induces translocation of GLUT4 and increases glucose uptake in muscle cells and adipocytes [32–36]. Insulin increases blood flow in muscle and adipose tissue via NO, resulting in an increase in glucose uptake in these tissues [37–39]. Additionally, NO mediates mitochondrial biogenesis and increases energy expenditure in adipose tissue, resulting in glucose consumption [40,41]. Because of these important functions of NO, it is not surprising that total absence of eNOS in knockout mice can affect metabolism [42–45]. What is surprising is that the single amino acid substitution of SA has profound effects that mimic eNOS knockout mice in the setting of completely normal eNOS protein levels and basal enzymatic activity. In contrast, SD mice fed a high fat diet maintain insulin sensitivity and have a lean phenotype. These results indicate that eNOS phosphorylation state and its regulation play important roles in insulin sensitivity.

We previously showed that modulation of eNOS phosphorylation, using a different transgenic approach, affects outcome to an intact animal model of stroke [30]. We also showed that the defective postnatal angiogenesis characteristic of Akt1 knockout mice was rescued by a phosphomimetic eNOS SD mutation [46]. The current report is the first demonstration that eNOS phosphorylation may be a therapeutic target for obesity and metabolism. Our results show that single amino acid modulation of the eNOS S1176 phosphorylation site alone is sufficient to affect systemic insulin sensitivity. Mice carrying the unphosphorylatable SA mutation display insulin resistance and features of metabolic syndrome, while mice carrying the phosphomimetic SD mutation show decreased insulin levels and resistance to high fat induced weight gain. Together, these results demonstrate a crucial role for eNOS phosphorylation in the mechanisms of metabolic diseases, and suggest that eNOS phosphorylation may be a useful target for treatment of diabetes and obesity.

References

[1] K.G. Alberti, P.Z. Zimmet, Definition, diagnosis and classification of diabetes mellitus and its complications, Diabet. Med. 15 (1998) 539–553.
[2] P.L. Huang, eNOS, metabolic syndrome and cardiovascular disease, Trends Endocrinol. Metab. 20 (2009) 295–302.
[3] P.L. Huang, A comprehensive definition for metabolic syndrome, Dis. Models Mech. 2 (2009) 231–237.
[4] U. Hink, H. Li, H. Mollnau, et al., Mechanisms underlying endothelial dysfunction in diabetes mellitus, Circ. Res. 88 (2001) E14–E22.
[5] M.A. Gimbrone Jr., J.N. Topper, T. Nagel, et al., Endothelial dysfunction, hemodynamic forces, and atherogenesis, Ann. NY Acad. Sci. 902 (2000) 230–239; discussion 239–40.
[6] M.A. Gimbrone Jr., Endothelial dysfunction and atherosclerosis, J. Card. Surg. 4 (1989) 180–183.

[7] D.M. Dudzinski, J. Igarashi, D. Greif, et al., The regulation and pharmacology of endothelial nitric oxide synthase, Annu. Rev. Pharmacol. Toxicol. 46 (2006) 235–276.
[8] P.L. Huang, Z. Huang, H. Mashimo, et al., Hypertension in mice lacking the gene for endothelial nitric oxide synthase, Nature 377 (1995) 239–242.
[9] J.E. Freedman, R. Sauter, E.M. Battinelli, et al., Deficient platelet-derived nitric oxide and enhanced hemostasis in mice lacking the NOSIII gene, Circ. Res. 84 (1999) 1416–1421.
[10] P.J. Kuhlencordt, R. Gyurko, F. Han, et al., Accelerated atherosclerosis, aortic aneurysm formation, and ischemic heart disease in apolipoprotein E/endothelial nitric oxide synthase double-knockout mice, Circulation 104 (2001) 448–454.
[11] D.J. Lefer, S.P. Jones, W.G. Girod, et al., Leukocyte-endothelial cell interactions in nitric oxide synthase-deficient mice, Am. J. Physiol. 276 (1999) H1943–H1950.
[12] M. Moroi, L. Zhang, T. Yasuda, et al., Interaction of genetic deficiency of endothelial nitric oxide, gender, and pregnancy in vascular response to injury in mice, J. Clin. Invest. 101 (1998) 1225–1232.
[13] T. Murohara, T. Asahara, M. Silver, et al., Nitric oxide synthase modulates angiogenesis in response to tissue ischemia, J. Clin. Invest. 101 (1998) 2567–2578.
[14] P.L. Huang, Unraveling the links between diabetes, obesity, and cardiovascular disease, Circ. Res. 96 (2005) 1129–1131.
[15] Y. Wang, P.A. Marsden, Nitric oxide synthases: gene structure and regulation, Adv. Pharmacol. 34 (1995) 71–90.
[16] S.M. Bode-Boger, R.H. Boger, S. Kienke, et al., Elevated L-arginine/dimethylarginine ratio contributes to enhanced systemic NO production by dietary L-arginine in hypercholesterolemic rabbits, Biochem. Biophys. Res. Commun. 219 (1996) 598–603.
[17] J.P. Cooke, Does ADMA cause endothelial dysfunction?, Arterioscler Thromb. Vasc. Biol. 20 (2000) 2032–2037.
[18] F. Cosentino, S. Patton, L.V. d'Uscio, et al., Tetrahydrobiopterin alters superoxide and nitric oxide release in prehypertensive rats, J. Clin. Invest. 101 (1998) 1530–1537.
[19] P.W. Shaul, Regulation of endothelial nitric oxide synthase: location, location, location, Annu. Rev. Physiol. 64 (2002) 749–774.
[20] S. Dimmeler, I. Fleming, B. Fisslthaler, et al., Activation of nitric oxide synthase in endothelial cells by Akt-dependent phosphorylation, Nature 399 (1999) 601–605.
[21] D. Fulton, J.P. Gratton, T.J. McCabe, et al., Regulation of endothelium-derived nitric oxide production by the protein kinase Akt, Nature 399 (1999) 597–601.
[22] Z.P. Chen, K.I. Mitchelhill, B.J. Michell, et al., AMP-activated protein kinase phosphorylation of endothelial NO synthase, FEBS Lett. 443 (1999) 285–289.
[23] K. Hisamoto, M. Ohmichi, H. Kurachi, et al., Estrogen induces the Akt-dependent activation of endothelial nitric-oxide synthase in vascular endothelial cells, J. Biol. Chem. 276 (2001) 3459–3467.
[24] Y. Kureishi, Z. Luo, I. Shiojima, et al., The HMG-CoA reductase inhibitor simvastatin activates the protein kinase Akt and promotes angiogenesis in normocholesterolemic animals, Nat. Med. 6 (2000) 1004–1010.
[25] M. Montagnani, H. Chen, V.A. Barr, et al., Insulin-stimulated activation of eNOS is independent of Ca2+ but requires phosphorylation by Akt at Ser(1179), J. Biol. Chem. 276 (2001) 30392–30398.
[26] R.S. Scotland, M. Morales-Ruiz, Y. Chen, et al., Functional reconstitution of endothelial nitric oxide synthase reveals the importance of serine 1179 in endothelium-dependent vasomotion, Circ. Res. 90 (2002) 904–910.
[27] C. Vecchione, A. Maffei, S. Colella, et al., Leptin effect on endothelial nitric oxide is mediated through Akt-endothelial nitric oxide synthase phosphorylation pathway, Diabetes 51 (2002) 168–173.
[28] H. Chen, M. Montagnani, T. Funahashi, et al., Adiponectin stimulates production of nitric oxide in vascular endothelial cells, J. Biol. Chem. 278 (2003) 45021–45026.
[29] N. Ouchi, H. Kobayashi, S. Kihara, et al., Adiponectin stimulates angiogenesis by promoting cross-talk between AMP-activated protein kinase and Akt signaling in endothelial cells, J. Biol. Chem. 279 (2004) 1304–1309.
[30] D.N. Atochin, A. Wang, V.W. Liu, et al., The phosphorylation state of eNOS modulates vascular reactivity and outcome of cerebral ischemia in vivo, J. Clin. Invest. 117 (2007) 1961–1967.
[31] B.B. Kahn, J.S. Flier, Obesity and insulin resistance, J. Clin. Invest. 106 (2000) 473–481.
[32] T.W. Balon, J.L. Nadler, Evidence that nitric oxide increases glucose transport in skeletal muscle, J. Appl. Physiol. 82 (1997) 359–363.
[33] Y. Higaki, M.F. Hirshman, N. Fujii, et al., Nitric oxide increases glucose uptake through a mechanism that is distinct from the insulin and contraction pathways in rat skeletal muscle, Diabetes 50 (2001) 241–247.
[34] D. McGrowder, D. Ragoobirsingh, P. Brown, Modulation of glucose uptake in adipose tissue by nitric oxide-generating compounds, J. Biosci. 31 (2006) 347–354.
[35] D. Roy, M. Perreault, A. Marette, Insulin stimulation of glucose uptake in skeletal muscles and adipose tissues in vivo is NO dependent, Am. J. Physiol. 274 (1998) E692–E699.
[36] T. Tanaka, K. Nakatani, K. Morioka, et al., Nitric oxide stimulates glucose transport through insulin-independent GLUT4 translocation in 3T3-L1 adipocytes, Eur. J. Endocrinol. 149 (2003) 61–67.
[37] J.R. Petrie, S. Ueda, D.J. Webb, et al., Endothelial nitric oxide production and insulin sensitivity. A physiological link with implications for pathogenesis of cardiovascular disease, Circulation 93 (1996) 1331–1333.
[38] H.O. Steinberg, G. Brechtel, A. Johnson, et al., Insulin-mediated skeletal muscle vasodilation is nitric oxide dependent. A novel action of insulin to increase nitric oxide release, J. Clin. Invest. 94 (1994) 1172–1179.
[39] H.O. Steinberg, H. Chaker, R. Leaming, et al., Obesity/insulin resistance is associated with endothelial dysfunction. Implications for the syndrome of insulin resistance, J. Clin. Invest. 97 (1996) 2601–2610.
[40] E. Nisoli, E. Clementi, S. Moncada, et al., Mitochondrial biogenesis as a cellular signaling framework, Biochem. Pharmacol. 67 (2004) 1–15.
[41] E. Nisoli, E. Clementi, C. Paolucci, et al., Mitochondrial biogenesis in mammals: the role of endogenous nitric oxide, Science 299 (2003) 896–899.
[42] H. Duplain, R. Burcelin, C. Sartori, et al., Insulin resistance, hyperlipidemia, and hypertension in mice lacking endothelial nitric oxide synthase, Circulation 104 (2001) 342–345.
[43] R.R. Shankar, Y. Wu, H.Q. Shen, et al., Mice with gene disruption of both endothelial and neuronal nitric oxide synthase exhibit insulin resistance, Diabetes 49 (2000) 684–687.
[44] S. Cook, O. Hugli, M. Egli, et al., Partial gene deletion of endothelial nitric oxide synthase predisposes to exaggerated high-fat diet-induced insulin resistance and arterial hypertension, Diabetes 53 (2004) 2067–2072.
[45] S. Cook, O. Hugli, M. Egli, et al., Clustering of cardiovascular risk factors mimicking the human metabolic syndrome X in eNOS null mice, Swiss Med. Wkly. 133 (2003) 360–363.
[46] M. Schleicher, J. Yu, T. Murata, et al., The Akt1-eNOS axis illustrates the specificity of kinase-substrate relationships in vivo, Sci. Signal. 2 (2009) ra41.